An advanced integrated avalanche photodiode with Si and Ge material

Wei Jiatong[1], Chen Liwei[1], Hu Haifan[1,2], Liu Zhiyuan[3]

(1. College of Information and Communication Engineering, Harbin Engineering University, Harbin 150001, China;
2. Nuctech Company Limited, Beijing 100084, China;
3. The 49th Research Institute of China Electronics Technology Group Corporation, Harbin 150001, China)

Abstract: An advanced avalanche photodiode (APD) was put forword which was integrated by the Si Separate Absorption, Charge, Multiplication (SACM) and Ge SACM APDs. This advanced APD has enlarged the detected wavelength range to 200-1 400 nm. Furthermore, the key parameters which were used to characterize the APD performance, such as the electric field distribution, the dark current and photocurrent, the gain, and the sensitivity of the APD were researched. The simulation results demonstrated that the breakdown voltage of the advanced APD is 145 V, the peak response is 22 A/W at 900 nm wavelength as cathode is 140 V, and the current gain of the advanced APD could get 50 at 400 nm wavelength before breakdown. The fabrication process was also discussed.

Key words: avalanche photodiode; wavelength region; device simulation

CLC number: TN364.2 **Document code:** A **DOI:** 10.3788/IRLA201645.S120002

基于硅与锗材料的改进集成雪崩光电二极管

魏佳童[1],陈立伟[1],胡海帆[1,2],刘志远[3]

(1. 哈尔滨工程大学 信息与通信工程学院,黑龙江 哈尔滨 150001;
2. 同方威视技术股份有限公司,北京 100084;
3. 中国电子科技集团公司第四十九研究所,黑龙江 哈尔滨 150001)

摘 要: 提出了一种改进的集成雪崩光电二极管器件结构，由硅和锗材料的雪崩光电二极管结构集成，分别包含吸收区、电荷区和倍增区结构。该改进雪崩光电二极管对光线波长的探测范围扩展到200~1 400 nm。对雪崩光电二极管的关键参数,如器件内电场分布、暗电流、光电流、增益和光响应等进行了分析。仿真结果表明改进雪崩光电二极管的击穿电压为 145 V。当阴极偏置电压为 140 V 时,该器件对 900 nm 波长光线的峰值响应可以达到 22 A/W。在器件击穿之前,400 nm 波长光线的电流增益可以对达到 50。对改进雪崩光电二极管器件的工艺流程也进行了讨论。

关键词: 雪崩光电二极管; 波长范围; 器件仿真

收稿日期:2016-02-01; **修订日期:**2016-03-20

基金项目:黑龙江省自然科学基金(F201413);中央高校基本科研业务费专项资金(HEUCF130818)

作者简介:魏佳童(1990-),女,硕士生,主要从事同时电子信息技术与光电器件方面的研究。Email:13946025949@163.com

导师简介:陈立伟(1974-),女,副教授,博士,主要从事信号与信息处理方面的研究。Email:chenliwei@hrbeu.edu.cn

通讯作者:胡海帆(1984-),男,讲师,博士,主要从事物理电子学与现代光电器件方面的研究。Email: huhaifan1@163.com

0 Introduction

The explosive spread of the internet has increased the demand for highly sensitive optical detectors for high bit rate optical fiber communication systems[1-2]. The avalanche photodiode (APD) is now finding acceptance in an increasing range of applications including optical communications, ranging, and laser systems[3-5]. Its advantages lie in its small size, internal current gain, high-frequency response, and it usually requires a relatively low supply voltage[6]. The materials used in APD structure have a major effect on determining the characteristics of the avalanche photodiode. There are three main materials used in avalanche photodiodes, germanium, silicon and group III -V compounds. Germanium can be used for wavelengths in the region of 800 -1 700 nm, and silicon can be used for wavelengths in the region between 200-1 100 nm[7]. Basic silicon photodiodes are very suitable for optical receivers because of their small capacitance and low dark current noise. However, the silicon avalanche photodiode is limited to use in the light detection between 400 nm to 900 nm due to its band gap characteristics[2].

In order to extend the wavelength range for APD, and make it effectively detect the wavelength in 200-1 400 nm, we investigate an integrated APD with Si and Ge material (IASG) to enhance its generality and enlarge its application field. Figure 1 gives the schematic diagram of the IASG. The IASG sandwiches a Si separate absorption, charge, multiplication(SACM) APD and a Ge SACM APD with an oxide layer. Here, the Si SACM APD is used to detect the light with wavelength in 200-1 000 nm, and the Ge APD is used to detect the light with wavelength in 900-1 400 nm. Si and Ge APDs are back-to-back. The anodes are led out from the top and bottom respectively, and the common cathode is leaded out by the N+ polysilicon. In addition, the N+ layer of Ge APD is formed by the $Si_{1-x}Ge_x$ material for reducing the process difficulty.

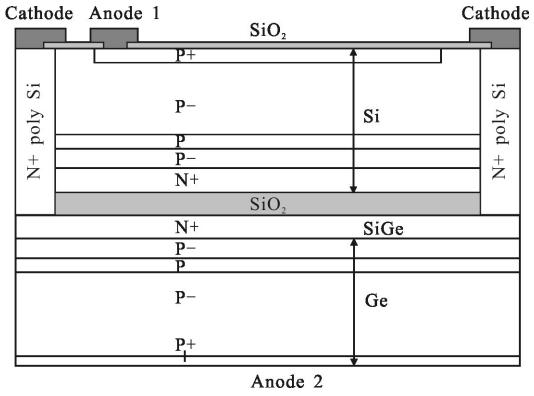

Fig.1 Schematic diagram of the IASG

1 Device structure and principle operation

Figure 2 shows the schematic diagram of avalanche process for IASG. The Antireflection (AR) Coating is used to decrease the reflecting of short wavelength light[9]. The long wavelength photons would go through the Si APD and be aborted by Ge APD,

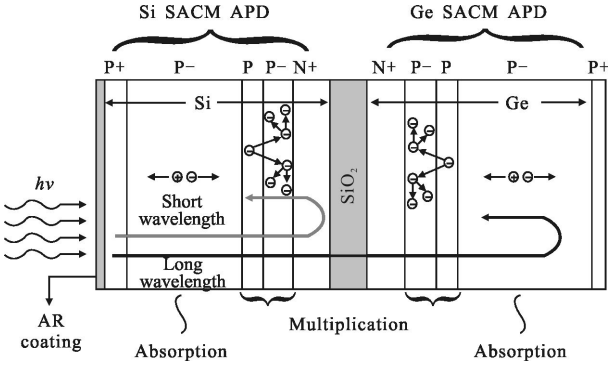

Fig.2 Schematic diagram of avalanche process for IASG

and the photon avalanche process for Ge APD is the same as that of Si APD. Because the P- silicon layer absorbing the photon has wavelengths in the range of approximately 200-1 100 nm [10]. Most of the light with wavelengths greater than approximately 1 100 nm is propagated through the Si SACM APD into the P- germanium layer of the absorption region. The P- germanium of layer absorbs that remaining light that propagates through layer up to wavelengths of approximately 1 400 nm. Then the IASG could detect the light wavelength from 200 nm to 1 400 nm, and the short and long wavelength signals are outputted

from the top and bottom anodes respectively.

Table 1 gives the IASG structure parameters. For balancing the Si APD and Ge APD in the light detection, and simplifying the bias control for ionization state in APD, the breakdown voltages of both should be the same. Therefore, the Si and Ge APD structures are designed all the same, except the higher doping concentration of P layer at the multiplication region, because the breakdown field of Ge is lower than that of Si, and the higher doping concentration of P layer could increase the electric field at the place between P layer (multiplication) and P− layer (absorption). Furthermore, the N+ region of Ge APD is formed by the $Si_{1-x}Ge_x$ material. This is for meeting the manufacturing process, and the detail process flow would be discussed at the lateral study.

Tab.1 IASG structure parameters

Parameters	Si SACM APD thickness and doping	Ge SACM APD thickness and doping
P+ layer	0.1 μm/1.0×10^{19} cm^{-3}	0.1vm/1.0×10^{19} cm^{-3}
P− layer (absorption)	30 μm/1.3×10^{14} cm^{-3}	30 μm/1.3×10^{14} cm^{-3}
P layer (Multiplication)	0.1 μm/2.0×10^{17} cm^{-3}	0.1 μm/2.5×10^{17} cm^{-3}
P− layer (Multiplication)	0.4 μm/5.0×10^{14} cm^{-3}	0.4 μm/5.0×10^{14} cm^{-3}
N+ layer	0.5 μm/2.0×10^{19} cm^{-3}	0.5 μm/2.0×10^{19} cm^{-3}
N+ Polysilicon	31.5 μm/2.0×10^{19} cm^{-3}	
Buried Oxide	0.5 μm	

2 Device characteristic and discussion

To study and discuss the IASG characteristics, a series of simulations were performed using the Silvaco TCAD software package [11−12]. The IASG structure is created by the Devedit simulator; then, the physical level equations and computing results were respectively conducted by ATLAS and analyzed by Tonyplot. The current gain is defined as the ratio of the cathode current and the effective photocurrent. Here, the light intensity is 1 W/cm^2 and the wavelength is 1.3 μm. Figure 3 shows the dependence of gain on reverse bias voltage for IASG as wavelength is 1.3 μm. the results illustrate that the tendency of current gain is the same as that of photoelectric current, and the gain increases quickly at the 145 V as IASG avalanche breakdown.

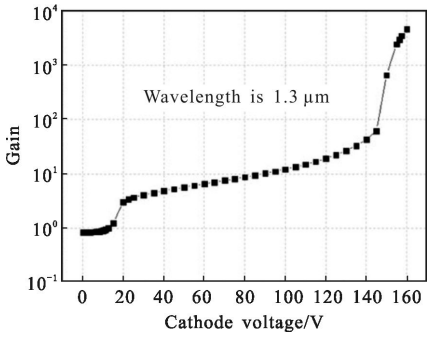

Fig.3 Dependence of gain on reverse bias voltage for IASG

Figure 4 gives the relationship between cathode current and wavelength for Si and Ge APDs as cathode voltage is 140 V. From the results we know that the photoelectric current of Si APD is in the region of 200 nm to 1 100 nm, and that of Ge APD is in the region of 800 nm to 1 600 nm. Si and Ge APDs have the same breakdown voltage, the ionization coefficient of Ge is higher than that of Si, but the AR coating is better for short wavelength photon, and would reflex part of long wavelength photon. Therefore, the Si APD has larger photoelectric current, while the Ge APD has expanded the detected light wavelength region for IASG.

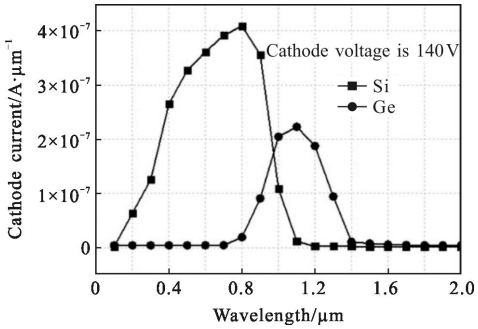

Fig.4 Relationship between cathode current and wavelength for Si and Ge APDs

The spectral sensitivity(R) of photodiode detector is defined as the ratio of the photoelectric current and

the input light power, and it could be expressed as [13]:

$$R=\frac{q\lambda}{hv}QE \tag{1}$$

Where, QE is the quantum efficiency, q is the electronic charge, λ is the light wavelength, and hv is the photon energy. QE is defined as the percentage of incident photons (I_{photon}) generating electron-hole pairs which subsequently contribute to the output current (I_{out}), and it could be expressed as[14]:

$$QE=I_{out}/I_{photon} \tag{2}$$

Figure 5 shows the impact of cathode voltage on the sensitivity and gain in the light region of 100 nm to 2 000 nm. The results show that the IASG has the wide wavelength region from 200 nm to 1 400 nm. The IASG has the peak response wavelength at 900 nm, and gets the highest gain at 400 nm. In the SACM APD detector, the hole generated in the N+ layer and the

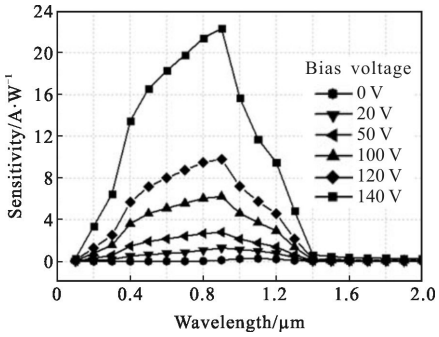

(a) Spectral sensitivity

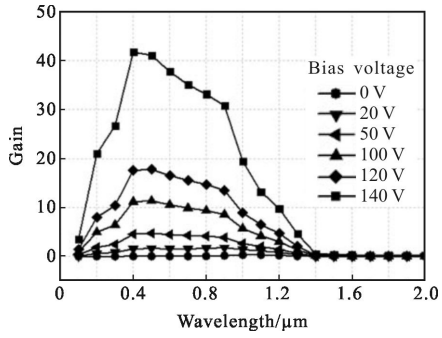

(b) Gain

Fig.5 Impact of cathode voltage on the sensitivity and gain

electron generated in the P− layer (multiplication region) by the photon would join in the multiplication. Because the ionization coefficient of electron is larger than that of hole, so the thickness of N+ layer is designed as 0.5 μm to get more electron in the avalanche multiplication.

Figure 6 gives the dependence of dark current on reverse bias voltage as different Ge content in $Si1_{-x}Ge_x$ layer for IASG detector[15]. In the IASG process flow, the Ge material is deposited on the $Si_{1-x}Ge_x$ layer for decreasing the defects at the interface of heterojunction, because the increasing Ge content could decrease the lattice mismatch between $Si_{1-x}Ge_x$ layer and Ge layer. The results in Fig.6 show that the dark current decreases with the increase of Ge content in $Si_{1-x}Ge_x$ layer. Here, x=0 represents that the $Si_{1-x}Ge_x$ layer is Si layer, and x=1 represents that the $Si_{1-x}Ge_x$ layer is Ge layer. Considering the process difficulty, the x=0.5 is used in the $Si_{1-x}Ge_x$ layer at Ge APD.

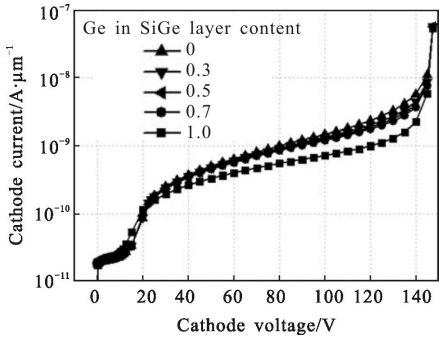

Fig.6 Dependence of dark current on reverse bias voltage as different Ge content in $Si_{1-x}Ge_x$ layer

The capacitance of APD is similar with that of photodiode, and the capacitance could be seen as a parallel plate capacitor, it is expressed as:

$$C=\frac{\varepsilon_r A}{4k\pi d} \tag{3}$$

Where, ε_r is the dielectric constant, A is the overlap area, and d is the space between the anode and cathode parallel plates. Figure 7 gives the capacitance comparison between Si APD, Ge APD and IASG. As cathode exceeds 20 V, the absorption region is depleted, and the multiplication region is depleted fully as cathode is larger than 80 V. So the space between the anode and cathode is the same for Si APD and Ge APD. Due to the dielectric constant of Ge and $Si_{0.5}Ge_{0.5}$ is bigger than that of Si, and the

overlap area of Ge APD is larger than that of Si APD, so the capacitance of Si APD is lower than that of Ge APD. Because the IASG structure consists of Si APD and Ge APD in parallel, therefore, the capacitance of IASG is the sum of the Si and Ge APDs.

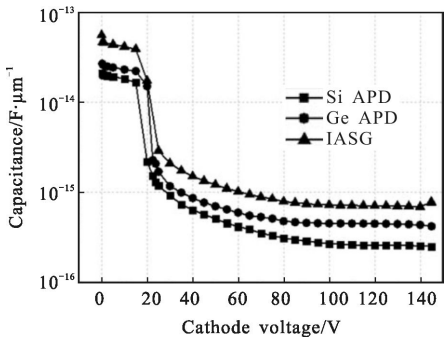

Fig.7 Dependence of capacitance on reverse bias voltage

3 Fabrication procedure

A sketch of the fabrication procedure of the SWBI pixel structure is illustrated in Fig.8(a). An P− doped SOI wafer *A* is prepared, and a thin P doped layer and a thin P− doped layer are deposited on the SOI wafer A. Meanwhile, a second SOI wafer B is prepared in Fig.8 (b). The top silicon layer used for cathode of Si APD is doped as N+ type. In Fig.8(c), the wafer *A* is turned over and bonded to the top of wafer *B*. *A* lithographically patterned P+ anode layer is formed on the top. In Fig.8 (d), the handled silicon of the SOI wafer *B* is polished to leave 0.5 μm Si layer. After the Ge and phosphorus implanted and annealing, an N+ doped SiGe layer is formed. In Fig.8(e), a thin P− doped Ge layer, a thin P doped Ge layer, a thick P− doped Ge layer and a thin P+ doped Ge layer are deposited on the SiGe layer in turn. Then, the Si APD and Ge APD are formed. In Fig.8 (f), a lithographically patterned trench is formed on the top, after the Si and oxide is etched to the SiGe layer, the

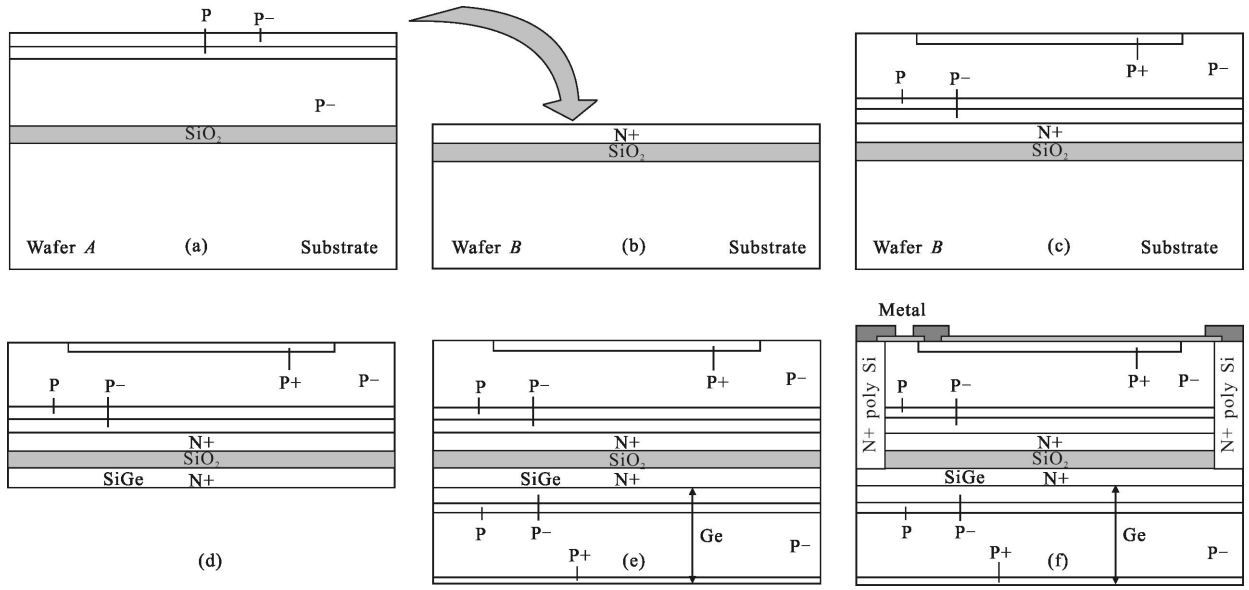

Fig.8 Main process for the fabrication of the IASG

polysilicon is deposited to fill and etched back to the Si surface. A thin oxide or nitride layer used for AR coating is deposited on the Si surface. Then, the top and bottom electrodes are formed.

4 Conclusion

To extend the wavelength range for APD, and make it effectively detect the wavelength in 200−

1 400 nm, an integrated APD with Si and Ge (IASG) is investigated to enhance its generality and enlarge its application field. The IASG is sandwiched a Si SACM APD and a Ge SACM APD with an oxide layer to detect the light of short and long wavelength respectively. The characteristics of IASG are studied, the simulation results demonstrated that the breakdown voltage of IASG is 145 V, the peak response is 22 A/W at 900 nm wavelength as cathode is 140 V, and the current gain of IASG could get 50 at 400 nm wavelength before breakdown.

References:

[1] Luo Q H, Yan X Z, Li J B, et al. DDEUDSC: Dynamic distance estimation using uncertain data stream clustering in mobile wireless sensor networks [J]. ***Measurement***, 2014, 55: 423-433.

[2] Luo Q H, Peng Y, Peng X Y. Uncertain data clustering-based distance estimation in wireless sensor networks [J]. ***Sensors***, 2014, 14: 584-6605.

[3] Mohd O, Siti T, Mohd H, et al. Reviews on avalanche photodiode for optical communication technology [J]. ***ARPN Journal of Engineering and Applied Sciences***, 2014, 9: 35-44.

[4] Zhang D P, Wu C, Zhang R Z. Study on thermal effect of LD end-pumped separated amplifier structure [J]. ***Infrared and Laser Engineering***, 2015, 44 (7): 2250 -2255. (in Chinese)

[5] Wang X, Xu Y J, Fan X G. Thermal performance testing for high power light-emitting diode based on voltage-current characteristics with pulse injection [J]. ***Infrared and Laser Engineering***, 2015, 44(8): 2417-2422.(in Chinese)

[6] Rochas A, Pauchard A R, Besse P A. Low-noise silicon avalanche photodiodes fabricated in conventional CMOS technologies [J]. ***IEEE Trans Elect Dev***, 2002, 49: 387-394.

[7] City F, Hayes J M, Corbett B. Modeling the effects of interface traps on the static and dynamic characteristics of Ge/Si avalanche photodiodes [J]. ***IEEE J Quantum Electronics***, 2011, 47: 849-857.

[8] Sze S M, Ng K K. Physics of Semiconductor Device [M]. 3rd ed. Hoboken: Wiley, 2007: 457-462.

[9] Wegrzecka I. Design and properties of silicon avalanche photodiodes [J]. ***Opto-Electrons Rev***, 2004, 12: 95-104.

[10] McIntyre R J, Webb P P, Dautet H. A short-wavelength selective reach-through avalanche photodiode [C]//Conference of NSSM, 1995, 1: 188-191.

[11] Silvaco International Software. Atlas user′s manual [Z]. Santa Clara, CA, USA, Silvaco: 2012.

[12] Silvaco International Software. Devedit user′s manual [Z]. Santa Clara, CA, USA, Silvaco: 2012.

[13] Ruegg H W. An optimized avalanche photodiode [J]. ***IEEE Trans Elect Dev***, 196, 5: 239-251.

[14] Jung S, Moon M, Kim H J. A simulation study of silicon avalanche photodiodes[C]//Conf of NSSM, 2006: 1064-1067.

[15] Michel J, Liu J, Kimerling L C. High-performance Ge-on-Si photodetectors [J]. ***Nature Photonics***, 2010, 4: 527-534.